The Astrophysical Journal, 668:533–545, 2007 October 10

TRIGGERING MECHANISM FOR THE FILAMENT ERUPTION ON 2005 SEPTEMBER 13 IN NOAA ACTIVE REGION 10808

Kaori Nagashima,[1,2,3] Hiroaki Isobe,[4] Takaaki Yokoyama,[4] Takako T. Ishii,[2]
Takenori J. Okamoto,[2] and Kazunari Shibata[2]
Received 2007 February 28; accepted 2007 June 23

ABSTRACT

On 2005 September 13 a filament eruption accompanied by a halo coronal mass ejection (CME) occurred in the most flare-productive active region, NOAA 10808, in solar cycle 23. Using multiwavelength observations before the filament eruption on September 13, we investigate the processes leading to the catastrophic eruption. We find that the filament slowly ascended at a speed of 0.1 km s^{-1} over 2 days before the eruption. During slow ascension, many small flares were observed close to the footpoints of the filament, where new magnetic elements were emerging. On the basis of the observational facts, we discuss the triggering mechanism leading to the filament eruption. We suggest that the process toward the eruption is as follows. First, a series of small flares played a role in changing the topology of the loops overlying the filament. Second, the small flares gradually changed the equilibrium state of the filament and caused the filament to ascend slowly over 2 days. Finally, a C2.9 flare that occurred when the filament was close to the critical point for loss of equilibrium directly led to the catastrophic filament eruption right after it.

Subject headings: Sun: coronal mass ejections (CMEs) — Sun: filaments — Sun: flares

Online material: mpeg animation

1. INTRODUCTION

Investigating the triggering mechanism of filament eruption is one of the most important subjects in the field of space weather, because such ejections of plasma and magnetic fields from the Sun lead to a significant disturbance of the magnetosphere and affect human life. It is widely accepted that flares, filament eruptions, and CMEs are different aspects of the same physical process, including plasma ejection and magnetic energy release (see Shibata et al. 1995; Forbes 2000). Several precursor signatures were reported (Martin 1980). However, what directly triggers such catastrophic eruptive events is not yet understood. Many theoretical models have been proposed (e.g., Moore & Roumeliotis 1992; Antiochos et al. 1999). As a catastrophe model for CMEs, Forbes (1990) and Forbes & Isenberg (1991) proposed the loss of equilibrium. Using a two-dimensional numerical simulation, Forbes (1990) confirmed that when the filament current exceeds a critical value, the stable configuration containing the filament loses equilibrium. When equilibrium is lost, the filament is magnetically driven upward and may evolve into a CME. Chen & Shibata (2000) and Lin et al. (2001) proposed the emerging flux-triggering mechanism for filament eruptions and CMEs, motivated by the observed correlation between reconnection-favored emerging flux and CMEs (e.g., Feynman & Martin 1995; Wang & Sheeley 1999).

From an observational point of view, however, conclusions reported in the literature have not yet converged regarding which model best explains the triggering mechanism of eruptive events. Therefore, accumulation of detailed analyses of individual events is still necessary in order to understand the physical mechanisms of solar eruptions, as well as to construct empirical models toward space weather forecast. In order to extract the essential physics and to compare with the existing theories, those events whose magnetic configuration is as simple as possible may be suitable. On the other hand, flare-productive active regions usually have very complex magnetic structures. From the viewpoint of space weather, we wish to understand and predict the eruptions from such complex active regions.

Therefore, in this paper we focus on the eruptive events in NOAA Active Region 10808, which appeared in 2005 September and showed the most furious flare activity during the current solar cycle (cycle 23). To have a clear view of the mechanism of the filament eruption in this region, we examined extensively the observational signatures that may lead to the filament eruption, using various available data. We find several interesting features that might help us to understand the physical mechanism of the eruption. One of those is that the filament that erupted on September 13 gradually deviated from the magnetic neutral line over 2 days. The speed of this ascending motion is approximately 0.1 km s^{-1}. Another feature is the sites where C- and M-class flares occurred during the period of ascending motion. In these sites magnetic elements emerged and moved markedly. We discuss a plausible triggering mechanism of the eruption, considering these features to be the clues. Independent analyses of this filament eruption were carried out by Chifor et al. (2007) and Wang et al. (2007).

In § 2 we give an overview of NOAA Active Region 10808. We describe the observations of a filament eruption that occurred on 2005 September 13 in § 3 and the long-time evolution of the filament in § 4. Discussions and conclusions are given in §§ 6 and 7, respectively.

2. OVERVIEW OF THE ACTIVE REGION

In 2005 September, a flare-productive active region appeared on the solar disk. NOAA Active Region 10808 appeared over the

[1] Department of Astronomy, Kyoto University, Sakyo-ku, Kyoto 606-8502, Japan.
[2] Kwasan and Hida Observatories, Kyoto University, Yamashina-ku, Kyoto 607-8471, Japan.
[3] Current address: Department of Astronomical Science, Graduate University for Advanced Studies (Sokendai), National Astronomical Observatory of Japan, 2-21-1, Osawa, Mitaka, Tokyo 181-8588, Japan; kaorin@solar.mtk.nao.ac.jp.
[4] Department of Earth and Planetary Science, University of Tokyo, Hongo, Bunkyo-ku, Tokyo 113-0033, Japan.

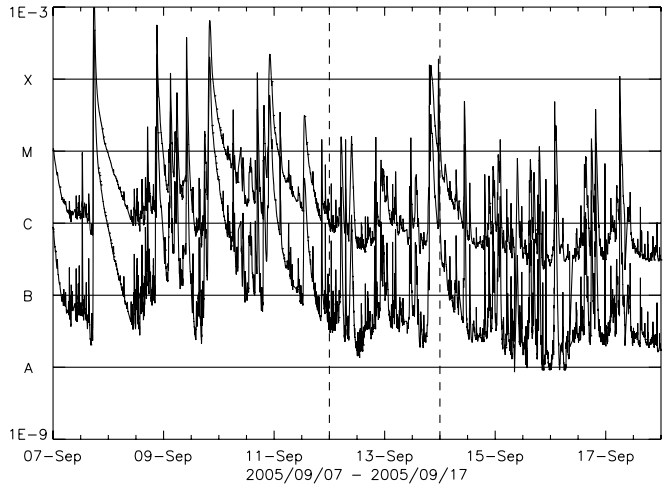

FIG. 1.—Soft X-ray fluxes in the *GOES* 0.5–4 Å (*lower*) and 1–8 Å (*upper*) channels from 2005 September 7 to 17. The data were obtained by *GOES-10*. In § 5 we focus on the M- and C-class flares that occurred during the period between the dashed lines (September 12 and 13).

east limb on 2005 September 7 and produced at least 10 X-class and 25 M-class flares until it disappeared behind the disk. Figure 1 shows the *Geostationary Operational Environmental Satellite* (*GOES*) soft X-ray light curve of the period when this active region was on the disk. Since no other strong active region was on the disk during this period, almost all the flares shown in this figure were attributed to this active region. This is the most intense flare activity during solar cycle 23, despite being in the declining phase of the cycle. After crossing the meridian the active region seemed to decay remarkably, and most of the X-class flares occurred in the eastern hemisphere. Some flares were accompanied by CMEs; however, they were not so geoeffective (see Wang et al. 2006).

It should be noted that this active region was the return of NOAA Active Region 10798 of the previous month. NOAA Active Region 10798 emerged into a coronal hole near the disk center and formed a sea-anemone-type active region (Shibata et al. 1994). By the time it rotated over the limb, two M-class flares accompanied by halo CMEs occurred and caused a large geomagnetic storm with a minimum Dst index of −216 nT (Asai et al. 2006).

In Figure 2, four sets of images show the evolution of the active region. Each set has a white-light image, photospheric magnetogram, and Hα image co-aligned with each other. The white-light images were taken by *Transition Region and Coronal Explorer* (*TRACE*; Handy et al. 1999). The magnetograms are those from the Michelson Doppler Imager (MDI; Scherrer et al. 1995) on board the *Solar and Heliospheric Observatory* (*SOHO*). The Hα images were clipped from the full-disk images obtained by the Solar Magnetic Activity Research Telescope (SMART; UeNo et al. 2004) at Hida Observatory, Kyoto University.

At the center of the active region was a delta-type sunspot that had two umbrae with different magnetic polarities packed tightly within a single penumbra. It showed a counterclockwise rotational motion. The direction of the motion was such that the orientation of the two polarities of the delta-type spot approaches the so-called Hale's polarity law (Hale et al. 1919). According to Hale's law, in the southern hemisphere the leading and following spots have negative and positive polarities, respectively, during solar cycle 23. The delta-type spot is surrounded by a more diffuse magnetic field that satisfies Hale's law. Running through the delta-type sunspot, there was an S-shaped neutral line in this active region (see Fig. 2; details are given in § 3). Along the neutral line, dark filaments were seen in Hα images in Figure 2. We find that when halo CMEs occurred on September 9, 11, and 13, the east part of the filaments erupted. Although the other halo CME occurred on September 10, we cannot identify the source region of the CME due to a lack of extreme-ultraviolet (EUV) and Hα data. Among these events, we focus on the filament eruption that occurred on September 13 to understand the mechanism of flares and their relationship to the processes of eruptive events in this active region.

3. FILAMENT ERUPTION ON 2005 SEPTEMBER 13

On 2005 September 13, an X1.5 class flare occurred near the disk center in NOAA Active Region 10808. This flare was accompanied by filament eruptions and a halo CME. A chronological description of the event is summarized in Table 1. Hereafter, this event is referred as the X1.5 event.

Figure 3 shows *GOES* soft X-ray light curves during this event. The *GOES* 1–8 Å flux began to increase at 19:19 UT and attained its peak at 19:27 UT. At the time of the *GOES* flux peak, two filaments erupted: the inner one (hereafter referred to as filament 2) brightened and erupted, and the outer one (referred to as filament 1) remained dark and seemed to ascend following filament 2. Figure 4 describes the motion of the filaments as they appeared in 195 Å images taken by *TRACE*.

Figure 5 shows the height-time profile for the erupting filaments along the slit shown in Figure 6*b*, as observed from *TRACE* 195 Å images. This height-time profile shows that filament 2 brightened and rapidly erupted at a velocity of 1.5×10^2 km s^{-1} (*white dot-dashed line*). Filament 1 remained dark and seemed to follow bright filament 2 at a speed of 5.8×10 km s^{-1} (*black dashed line*); the upward velocity increased up to 2.5×10^2 km s^{-1} (*white dashed line*). Such motions of the filaments are also recognizable in Figure 4.

Figure 6 explains the magnetic structure of the active region and the locations of the filaments and the flares. Figure 6*a* shows the *SOHO* MDI magnetogram overlaid on the *TRACE* 195 Å image before the eruption. In this region, there was an S-shaped neutral line running through the delta-type sunspot as shown in Figure 6*d*. The filament eruption occurred all along the southeast part of this neutral line. At the same time of the eruption, the flare core brightened in EUV on the east side of the delta-type sunspot along the neutral line; this region is labeled as region C (see Fig. 6*d*). Region C is characterized by several small negative-polarity magnetic elements moving one after another from the negative-polarity umbra in the delta-type spot (see Fig. 12 and § 5.2 for details). Another characteristic site in the magnetograms is on the opposite side of the neutral line from region C. In this region, hereafter referred to as region T, many magnetic elements flowed out near the neutral line (see Fig. 12 and § 5.3 for details). As discussed in § 5, many small (C- and M-class) flares occurred in regions C and T before the X1.5 event. These characteristic magnetic regions are summarized in Figure 6*f*, with their characteristic motions indicated by arrows. In this panel, filaments are indicated by gray lines: filament 1 (F1) originally appeared above the S-shaped neutral line and gradually deviated southeast, while filament 2 (F2) appeared above the neutral line by the time the X1.5 event occurred.

Although the initiation of the filament eruption was unclear in EUV because the *TRACE* satellite was in the South Atlantic Anomaly (SAA) during the period, the first flare brightening in the Hα blue wing (Hα − 0.6 Å) was observed right before the eruption of filaments 1 and 2. Figure 6*c* shows an Hα wing

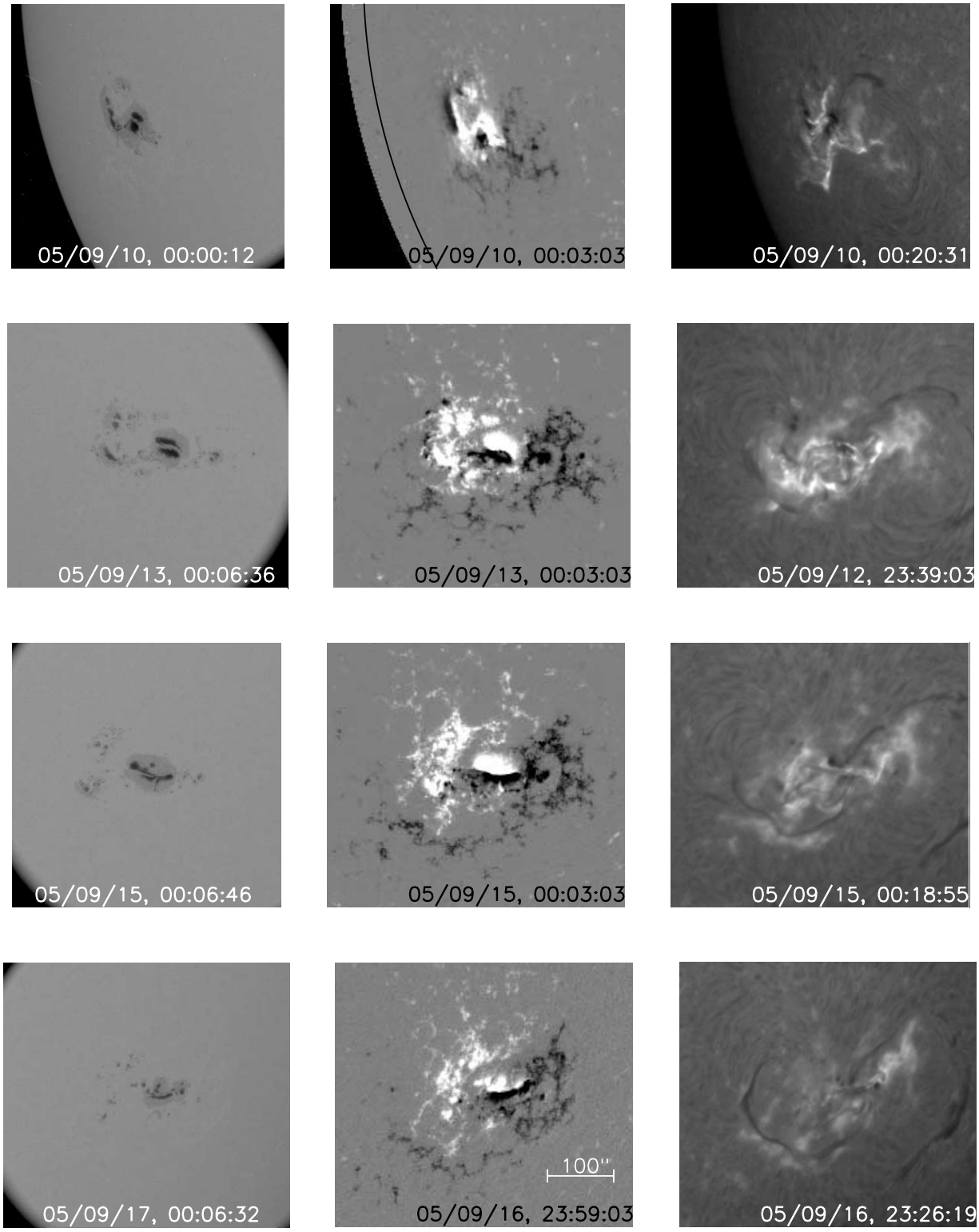

FIG. 2.—Evolution of NOAA Active Region 10808. *TRACE* white-light images, *SOHO* MDI magnetograms, and SMART Hα images are shown in the first, second, and third columns, respectively. In magnetograms, white and black indicate positive and negative polarities, respectively, and solid lines indicate the solar limb. The field of view of these images is $450'' \times 400''$. North is up, and west is to the right in these and other solar images in this paper.

(Hα − 0.6 Å) image taken at the Big Bear Solar Observatory (BBSO). The brightening began from region C, as shown in Figure 6*c*, and expanded southeast along the S-shaped neutral line. After the filament eruption, flare ribbons formed along the S-shaped neutral line, which are shown in *TRACE* 1600 Å images in Figure 6*e*.

After the filament eruption mentioned above, a fainter eruptive event occurred in the south part of the active region at around 20:00 UT, i.e., at the second peak of the *GOES* flux. Footpoints of this erupting filament were located west of the delta-type sunspot and close to the postflare loops southeast of the active region.

TABLE 1
TIMELINE SUMMARY OF THE 2005 SEPTEMBER 13 X1.5 EVENT

Time (UT)	Event
18:40	Brightening in region T begins (195 Å)
19:05	*GOES* soft X-ray flux peak at C2.9[a]
19:22	Brightening in region C (Hα − 0.6 Å)
19:24	Filament 1 begins to rise (Hα − 0.6 Å)
19:24	Filament 2 begins to brighten and rise (195 Å)
19:27	*GOES* soft X-ray flux first peak at X1.5
20:00	*GOES* second peak, faint eruption (195 Å)
20:00	Halo CME with a speed of 1866 km s^{-1} (LASCO C2)

[a] We consider this event a direct trigger of the filament eruption; see text.

These erupting events seemed to evolve into a white-light halo CME. According to the CME catalog[5] (Yashiro et al. 2004), this event is recognized as a halo CME with a projected speed of 1866 km s^{-1}. In *SOHO* LASCO C2 images, two blobs were observed; the second bright core is thought to be related to the second eruption at 20:00 UT, because its launch time is estimated at around that time on the basis of the linear extrapolation of its track.

4. LONG-TIME EVOLUTION OF FILAMENTS

Before the September 13 eruption (the X1.5 event), we can see two filaments in the southeast part of the active region: the outer one (filament 1) and the inner one (filament 2). They formed after another filament eruption on September 11. We concentrate on the evolution of these filaments after the eruption on September 11. We find that filament 1 continuously deviated from the neutral line from September 11 to 13. Figure 7 shows the time evolution of EUV intensity along the slit shown in Figure 6*b*. The solid line with asterisks indicates the position of the magnetic neutral line. This figure shows that the filament seemed to separate from the neutral line at a nearly constant speed of 0.12 km s^{-1} over more than 40 hours, while the filament accelerated to 200–300 km s^{-1} when it erupted as mentioned in § 3. Although we see only the plane-of-sky motion of the filament separating from the neutral line, we can interpret it as an ascending motion by taking into account the projection effect. Such a slow and long-lasting ascending motion is probably different from the so-called slow-rise phase of the erupting filaments, such as those reported by Ohyama & Shibata (1997; see also Kahler et al. 1988; Rompolt 1990; Zhang et al. 2001; Sterling & Moore 2004). Chifor et al. (2006) reported the early evolution of a prominence eruption observed on 2005 July 27. Slow rise at a speed of 4.8 km s^{-1} was observed over 30 minutes prior to the fast-rise phase during which the filament accelerated up to 300 km s^{-1}. Since the slow ascending motion continues much longer than those in the previously reported events, we believe the physical mechanism is different. Isobe & Tripathi (2006) and Isobe et al. (2007) reported an observation of slow-rising motion (1 km s^{-1}) of a polar crown filament that lasted for more than 10 hours before it finally erupted. They found a large-amplitude oscillation of the filament during the slow rising, and hence concluded that the filament retained a stable equilibrium and the rising motion is a quasi-static evolution. This may be the same phenomenon as our long-lasting slow rise. Existence of such long-term slow rise has been also pointed out by S. Martin (2007, private communication).

[5] See http://cdaw.gsfc.nasa.gov/CME_list/index.html.

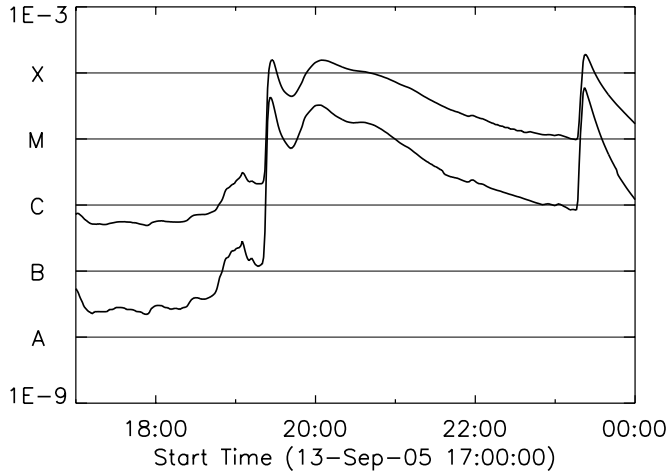

FIG. 3.—Soft X-ray fluxes in the *GOES* 0.5–4 Å (*lower*) and 1–8 Å (*upper*) channels on 2005 September 13.

It should be noted that filament 1 showed active motion along its axis in *TRACE* EUV images and SMART Hα images during its slow ascension, i.e., over 2 days (e.g., Martin 1980).

5. PREFLARE BRIGHTENINGS ON SEPTEMBER 12 AND 13

5.1. *All M- and C-class Flares*

During the slow rise of the filament, several M- and C-class flares and small brightenings in the EUV occurred in this active region. As shown between the dashed lines in Figure 1, five M-class and 18 C-class flares occurred since 00:00 UT on September 12 until the X1.5 flare on September 13. All of these flares are listed in Table 2, and the locations on the magnetogram are shown in Figure 8. These flares can be categorized into four groups: (I) eruptive events along the S-shaped neutral line (the X1.5 event), (II) brightenings around filaments on the east side of the delta-type spot (region C), (III) local events in the emerging flux region (region T), and (IV) small jets in the northeast part of the active region. Since small jets (group IV) were localized events and were not attributed to the S-shaped neutral line, we consider that these events did not have direct influence on the X1.5 event. *TRACE* 195 Å images of groups II, III, and IV are shown in Figure 9.

Group I is the filament eruption during the X1.5 event on September 13. We consider the other smaller events (groups II and III) that occurred along the S-shaped neutral line as a key to finding out the triggering mechanism of the X1.5 event. First, we focus on the events that occurred in region C (group II) to consider the eruptive process of the X1.5 event. Next, we consider the last local event (group III) right before the X1.5 event to consider the direct triggering mechanism of the X1.5 event.

5.2. *Filaments in Region C, and M1.5 and M6.1 Flares on September 12*

One of the puzzling points in the X1.5 event is that although the flare ribbon extended throughout the S-shaped neutral line, the filament was visible only in the southeast part of the neutral line. We suggest also that an eruptive process did occur in region C, although we did not observe a filament during the X1.5 event. The magnetic topology may be either a flux rope (e.g., Priest et al. 1989; Low 1996) or a sheared arcade (e.g., Antiochos et al. 1994).

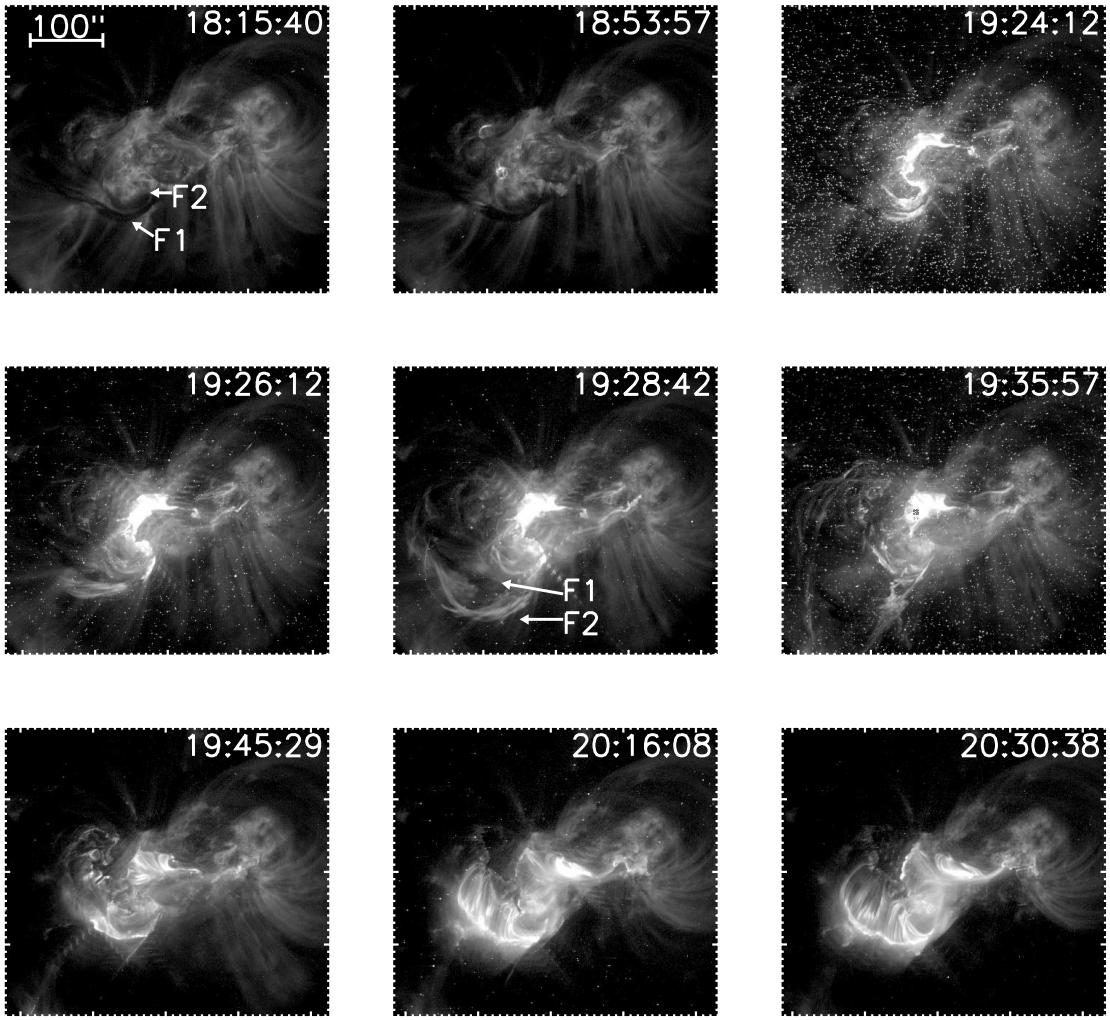

FIG. 4.— *TRACE* 195 Å images of NOAA Active Region 10808 before and during the X1.5 event on 2005 September 13. F1 and F2 indicate filaments 1 and 2, respectively (see text). The field of view is $450'' \times 400''$, the same as that in Fig. 2, and the ticks correspond to $10''$. [*This figure is available as an mpeg animation in the electronic edition of the Journal*.]

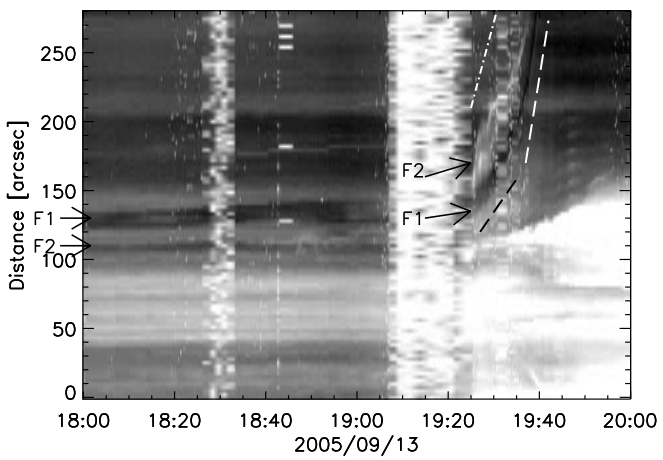

FIG. 5.— Time slice for the slit shown in Fig. 6*b*. The spatial slices are laid adjacent from left to right in the diagram. The distance is measured from the northwestern end of the slit. Arrows labeled as F1 and F2 point to filaments 1 and 2. The white dot-dashed line, white dashed line, and black dashed line indicate 1.5×10^2, 2.5×10^2, and 5.8×10 km s^{-1}, respectively.

A filament was actually visible in region C some time during September 12 and 13. An M1.5 flare occurred in region C at 5:05 UT on September 12. An EUV brightening seemed to be located under a dark filament in region C. Neither an eruption nor a CME was observed during this event. Some loops overlying the dark filament brightened after the main phase. Four hours after the M1.5 flare, an M6.1 class flare occurred at 9:03 UT. Figure 10 shows *TRACE* 195 Å images of this event. In this event, brightening in the EUV started from region C. A thin dark filament in region C was lifted up and seemed to erupt at 8:46 UT, i.e., the first peak of the *GOES* soft X-ray flux. The thin dark filament twined around the brightening loop. When the brightening loop expanded, the dark filament erupted. Although the dark filament could not be identified clearly after its eruption, according to the CME catalog (Yashiro et al. 2004), a narrow CME was observed by the *SOHO* Large Angle and Spectrometric Coronagraph Experiment (LASCO) right after this event. A little thin lump of bright coronal emission first appeared in the LASCO C2 field of view at 9:12 UT and was recognized as a CME with a projected speed of 511 km s^{-1}, which is consistent with the assumption that the filament erupted at around 8:46 UT and evolved into a CME.

After these flares, a dark filament existed in region C. This filament could be seen in SMART Hα wing (H$\alpha \pm 0.5$ Å) images

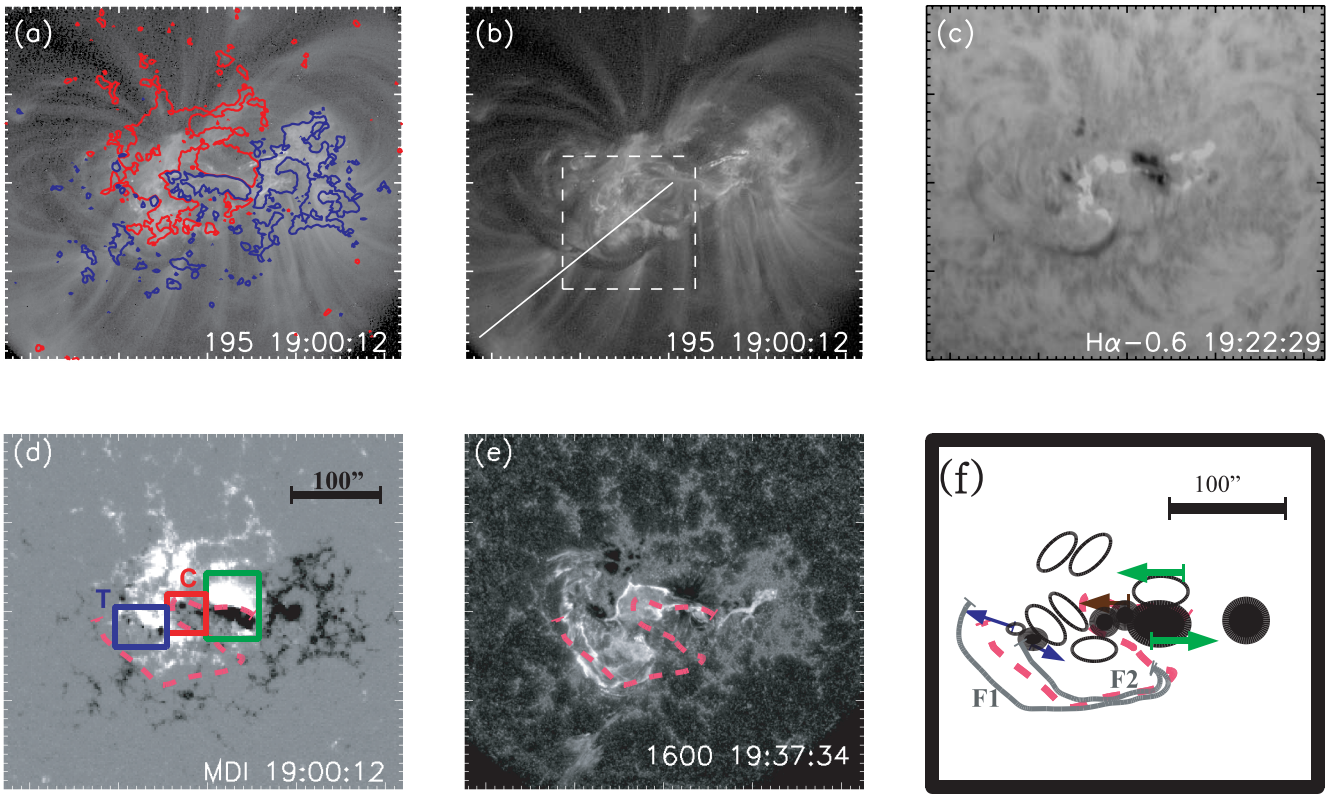

FIG. 6.—Magnetic structure of NOAA Active Region 10808. The field of view of these images except Fig. 6*f* is 450″ × 400″, the same as that in Fig. 2. A 100″ long scale that corresponds to about 7×10^4 km on the solar surface is shown in Fig. 6*d*. (*a*) *SOHO* MDI magnetogram contours superimposed on the *TRACE* 195 Å image. The *TRACE* 195 Å image was taken at 19:00:12 UT, and the magnetogram was taken at 19:11:03 UT. Displacement between these images due to a difference in time and pointing is corrected. Red and blue contours represent ±100 G. (*b*) *TRACE* 195 Å image. The solid line indicates the slit position of the time slice shown in Figs. 5 and 7. The dashed box indicates the field of view of a series of *TRACE* 195 Å images in Fig. 11 and of a series of magnetic maps shown in Fig. 12. (*c*) BBSO Hα wing (Hα − 0.6 Å) image of the active region before the X1.5 event. (*d*) *SOHO* MDI magnetogram. A green box indicates the delta-type sunspot, and a pink dashed line indicates the S-shaped neutral line. Region C in the red box and region T in the blue box are the sites where small flares occurred frequently. (*e*) *TRACE* 1600 Å image taken at 19:37:34 UT. A pink dashed line indicates the S-shaped neutral line. Flare ribbons appeared along the S-shaped neutral line. (*f*) Schematic illustration of this active region. In this panel, the central part of the active region is enlarged. White and black circles indicate positive and negative polarity regions, respectively. The meaning of the pink dashed line is the same as in Fig. 6*d*. Gray lines indicate filaments.

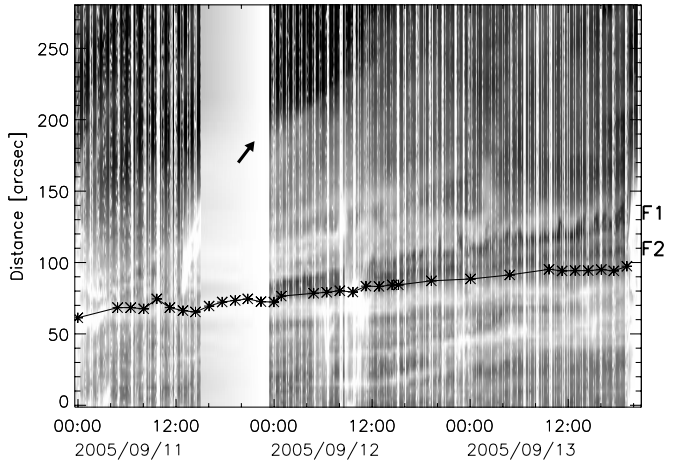

FIG. 7.—Time slice for the slit shown in Fig. 6*b*. The distance is measured from the northwestern end of the slit. The solid line with asterisks indicates the position of the magnetic neutral line. Asterisks are the data points. The error of the neutral line position is roughly 10″. F1 and F2 indicate dark filaments 1 and 2, respectively. The black arrow indicates the rising motion of a bright structure (see § 6).

taken at around 3:00 UT on September 13. We observed ceaseless mass flow along the filament in region C. This is similar to the active motion of filament 1 along its axis that is mentioned in § 4.

On the basis of the observational features of the small dark filament in region C, we speculate that there was a flux rope or sheared field in region C. Owing to the nonsteady mass flow along the filament in region C, the filament itself was sometimes visible and, another time, was invisible. However, the magnetic field that supported the filament should have existed all the time. Considering the fact that during the X1.5 event the brightening in Hα started from region C and extended to the southeast part, we suppose that this eruptive process in region C was the initiation of the X1.5 event even though the filament in region C was invisible at the time of the event. Those observations described in this section support the idea that a flux rope (or whatever plays the role of a filament) did exist in region C even at the time of the X1.5 event on September 13.

5.3. *Possible Direct Trigger for the X1.5 Event: C2.9 Flare on September 13*

A small brightening in the EUV close to the footpoint of filament 2 was observed 40 minutes before the filament eruption. It was recorded as a *GOES* C2.9 class flare at 19:05 UT (see Fig. 3). We consider this event as the final trigger of the X1.5 event.

TABLE 2
X-, M-, AND C-CLASS FLARES ON SEPTEMBER 12 AND 13

DATE	TIME[a]			*GOES* CLASS	CME	LOCATION [GROUP]
	Start	Peak	End			
Sep 12	00:45	00:49	00:53	C3.3	None	Region C [II]
	02:42	02:48	02:53	C2.0	None	Region C [II]
	04:49	05:05	05:27	M1.5	None	Region C [II]
	06:56	07:01	07:05	M1.3	None	Region T (failed eruption) [III]
	08:37	09:03	09:20	M6.1	CME	Region C (eruption) [II]
	15:33	15:37	15:42	C1.1	None	Region C [II]
	16:29	16:33	16:35	C1.1	None	Region T [III]
	16:35	16:38	16:40	C1.2	None	Region T [III]
	19:28	19:40	19:42	C3.2	None	Jet [IV]
	20:05	20:09	20:11	M1.5	None	Region T [III]
	22:07	22:25	22:42	C7.2	None	Region C [II]
	22:57	23:01	23:03	C5.6	None	To the southwest of delta-type spot
	23:12	23:17	23:23	C5.5	None	Region T [III]
Sep 13	00:53	00:58	01:02	C4.3	None	Region T [III]
	03:21	03:27	03:31	C3.4	None	Region T [III]
	03:57	04:00	04:02	C1.5	None	Jet [IV]
	04:15	04:18	04:20	C1.9	None	Region T [III]
	04:37	04:45	04:54	C5.1	None	Region T [III]
	06:31	06:35	06:37	C1.2	None	Region T [III]
	08:24	08:28	08:31	C1.8	None	Region T? [III?]
	10:41	11:21	11:24	M1.3	None	Region C [II]
	13:11	13:43	13:53	C4.5	None	Region C [II]
	18:49	19:05	19:15	C2.9	None	Region T [III]
	19:19	19:27	20:57	X1.5	Halo CME	Filament eruption along NL [I]
	23:15	23:22	23:30	X1.7[b]	CME	Above the delta-type spot

[a] The timescale of flares is based on the data of the *GOES* X-ray flux. See http://www.ngdc.noaa.gov/stp/SOLAR/ftpsolarflares.html.
[b] In this study, we do not refer to this event.

At the site of the C2.9 flare, successive appearances of small magnetic elements were seen in magnetograms. Figure 11 shows a series of *TRACE* 195 Å images during this event. *SOHO* MDI magnetogram contours are overlaid; red and blue contours indicate ± 100 G. At around the center of each panel, a small brightening in the EUV appeared, and jetlike features indicated by the white arrow were observed to the east of the bright loops. These dark jetlike features are also seen in BBSO Hα wing (Hα $-$ 0.6 Å) images. These jets and loops moved eastward gradually, and the jets also showed a whiplike motion. Moreover, on the left side of bright jetlike features, dark backward flows were observed when we check a *TRACE* 195 Å movie of this event (see mpeg animation of Fig. 4). Figure 12 shows a series of MDI magnetograms taken mainly on September 12 and 13. From the tail part of the S-shaped neutral line, many small magnetic elements were flowing out. Although region T was dominated by the negative polarity, patchy magnetic elements with both polarities were emerging. Over the 2 days before the filament eruption, similar small brightenings in the EUV that were identified as C- or sub-C-class flares by *GOES* occurred in similar locations (Fig. 8); C-class events are listed in Table 2. Taking a closer look at the sites of small brightenings, they moved slightly southward with time, but corresponded to the source region of the emerging mixed polarities.

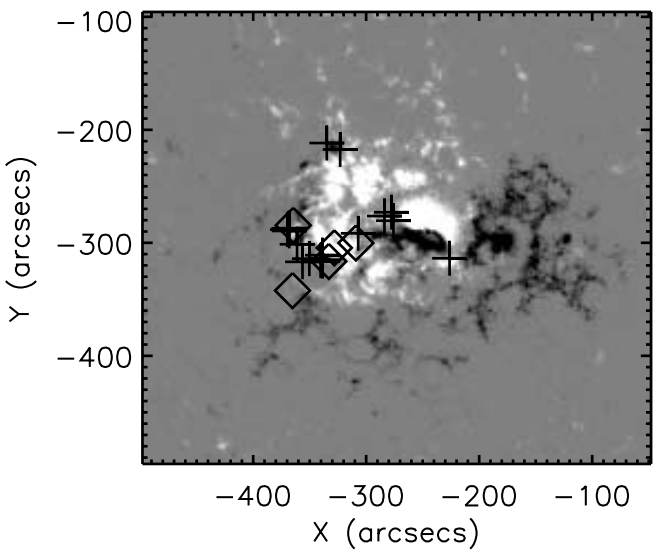

FIG. 8.—Location of the M- and C-class flares that occurred on 2005 September 12 and 13, shown by a *SOHO* MDI magnetogram. White and black indicate positive and negative polarities in the magnetogram, respectively. Diamonds and crosses indicate M class and C class, respectively. The field of view is the same as that in Fig. 2.

It is noteworthy that an element of negative polarity that first appeared in the frame taken at 19:15 UT on September 12 (Fig. 12, *top row, second panel*) moved southwest along the neutral line. It weakened the positive region so that the positive region divided into parts after the X1.5 event (see the magnetogram image taken at 14:27 on September 14 in Fig. 12). This negative element was located at the footpoint of the brightening loop during the C2.9 event at 19:05 UT on September 13. We examine the motion of the negative element, and it yields valuable clues to understanding the triggering mechanism of the X1.5 event (see § 6).

It should be noted that small brightenings in the EUV 195 Å were also found just before the X1.5 event on the west side of the delta-type spot. In Hα wing (Hα $-$ 0.6 Å) images taken at BBSO,

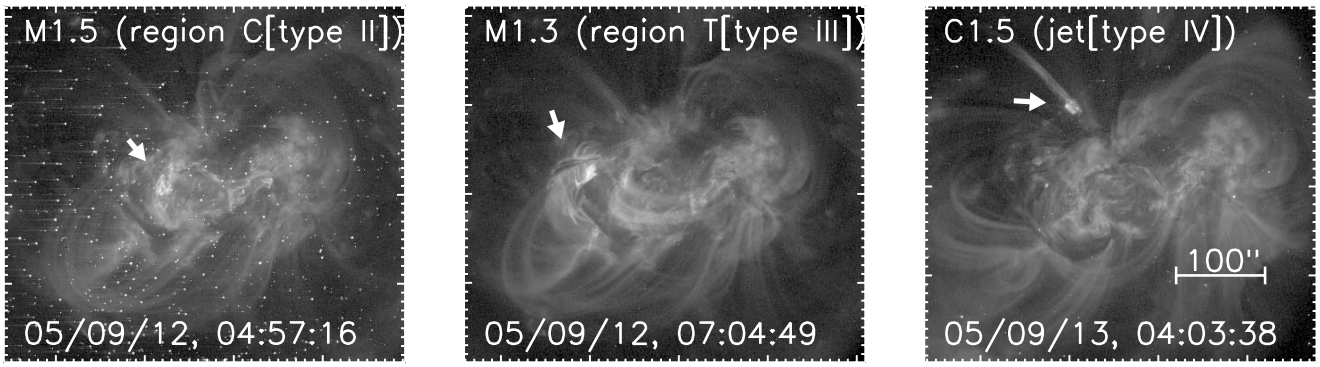

FIG. 9.— *TRACE* 195 Å images showing representative events of group II, III, and IV on 2005 September 12 and 13. Arrows indicate the sites of brightening. The field of view is the same as that in Fig. 2.

the only data taken simultaneously during this period, we cannot identify corresponding brightenings. Although this event occurred in the same period as the C2.9 event, we consider that this west-part event did not have a direct influence in triggering the X1.5 event. The reasons are as follows. (1) In this region, similar brightenings in the EUV were also observed 1 hour before this event. (2) The dark filament in this region seemed not to be affected by the X1.5 event, and remained as it was after the X1.5 event. (3) Although located close to the footpoint of the second eruption at around 20:00 UT, the magnetic field lines in this region did not seem to directly connect with those that were involved in the X1.5 event. Another brightening was observed to the northeast of the tail of the S-shaped neutral line (see Fig. 4, *top row, center panel*). We consider that this event was not directly related to the X1.5 event, for similar reasons.

6. DISCUSSION: TRIGGERING MECHANISM OF THE X1.5 EVENT

On the basis of the multiwavelength observations, we discuss the triggering mechanism of the X1.5 event. As mentioned in § 5, we considered M- and C-class flares on September 12 and 13 as a key to finding out the triggering mechanism of the X1.5 event.

A filament eruption occurred at 13:12 on September 11, accompanying an M3.0 flare. At least 10 hours after this filament eruption, another filament was reformed along the S-shaped neutral line. After that, several M- and C-class flares and small brightenings in the EUV occurred in region C and region T. We consider that these small flares played a role in lengthening the magnetic arcades overlying the filaments.

In region C, the negative elements flowed out from the negative part of the delta-type spot during September 12 and 13. When small flares occurred in region C, such as the M1.5 flare at 05:05 UT on September 12 and the M6.1 flare at 09:03 UT on September 12, the magnetic field lines connecting to these negative elements reconnected to the loops overlying the filaments in region C; a schematic illustration is shown in Figure 13. Note that the positive element on the left side of the pointed negative element shown in Figures 13*b*–13*d* was not in reality on line AB shown in Figure 13*a*; we consider that it was located on the positive side of the delta-type spot. During the events in region C, bright loops crossing over the dark filament were observed: this is evidence that the loops overlying the filament were involved in the reconnection process as shown in Figure 13. As mentioned in § 5.2, no eruption was observed during all but the M6.1 flare at 09:03 UT on September 12; the M6.1 flare was associated with a small filament eruption in region C, which appeared to evolve into a CME. We consider that most events only changed the equilibrium state of the filament in region C, while the perturbation at the time of the M6.1 flare was strong enough to trigger the eruption of the filament. However, we consider that all these flares in region C (group II events) occurred in essentially the same way as the mechanism shown in Figure 13.

As for the flares in region T (group III events), we interpret them in a similar way. Although group II and group III were apparently independent events, they were located along a single magnetic neutral line (the S-shaped neutral line; see Fig. 6*f*) in the active region. Moreover, during the X1.5 event, throughout the east part of the S-shaped neutral line, flare ribbons were observed. Therefore, we suppose that these filaments were different parts of one flux rope or sheared field along the S-shaped neutral line, and similar mechanisms for small flares along the neutral line (group II and III events) are suggested.

As the reconnection associated with these small flares lengthened overlying loops, the filaments changed its equilibrium state

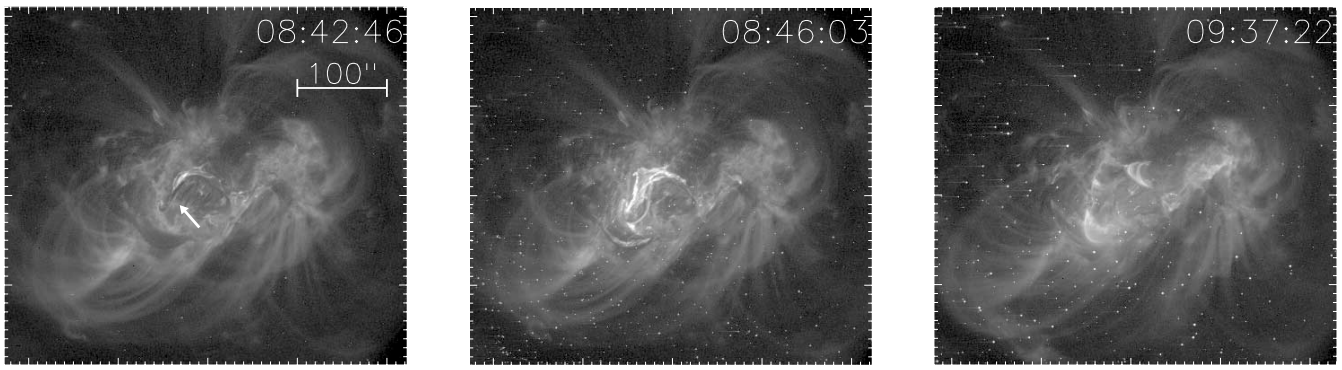

FIG. 10.— *TRACE* 195 Å images showing the filament eruption in region C. During the M6.1 class flare at 9:03 UT on September 12, the thin dark filament (*arrow in the left panel*) in region C appears to be lifted up by a brightening loop and erupted. The field of view of these images is the same as that in Fig. 2.

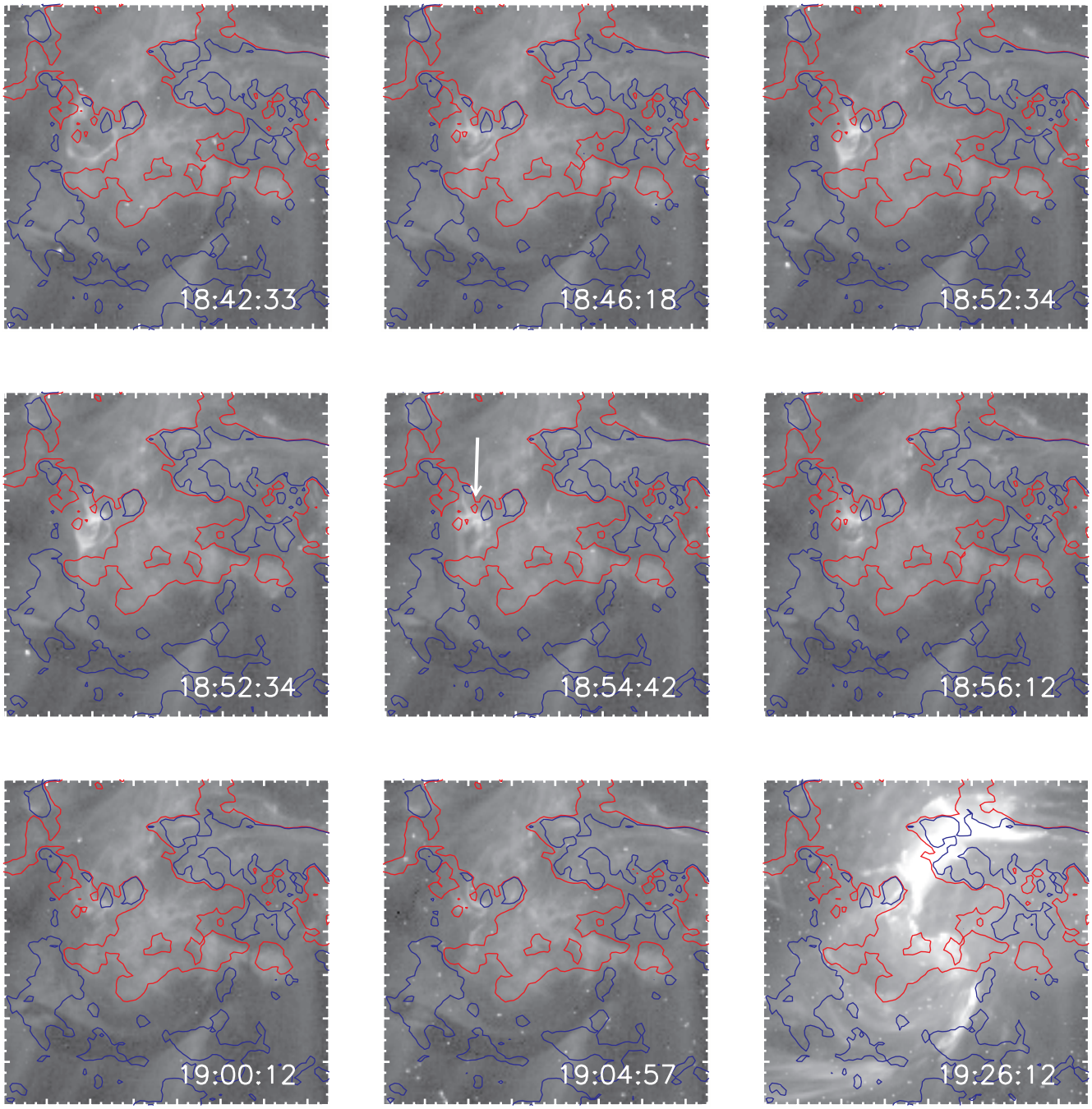

FIG. 11.—*SOHO* MDI magnetogram contours overlaid on *TRACE* 195 Å images, showing the C2.9 flare considered to be a trigger of the X1.5 event. The white arrow in the center panel indicates the jetlike feature. The bottom right panel shows the filament eruption during the X1.5 event (see Fig. 4), indicating the relative position against the C2.9 flare. Red and blue contours indicate +100 G and −100 G, respectively. The field of view of these images is shown in Fig. 6*b* as a dashed box and is 150″ square.

and appeared to deviate from the neutral line. Finally, the filaments erupted after the C2.9 flare that occurred at 19:05 UT on September 13 in region T. We suppose that this small flare was a direct trigger of the filament eruption (the X1.5 event). At that time the filaments were probably very close to the critical point for loss of equilibrium, and erupted as a result of the C2.9 flare. Magnetic configuration of the C2.9 flare on September 13 is shown in Figure 14. The emerging flux whose footpoint was located on the flowing negative element interacted with the loops overlying filament 2. The reconnected loop brightened, and a jetlike feature crossing over the filament was observed. This jetlike feature showed a whiplike motion as the magnetic reconnection proceeded.

The characteristic features observed during September 12 and 13 are summarized as follows. (1) Filament 1 continuously ascended slowly. (2) Many M- and C-class flares occurred around the footpoints of filaments; however, no eruption was observed during all but the M6.1 flare in region C on September 12. (3) Although the C2.9 flare on September 13 showed a similar magnetic structure to the preceding M- and C-class events and was not a strong event in particular, it seemed to trigger the catastrophic eruption (the X1.5 event). We suggest that a series of

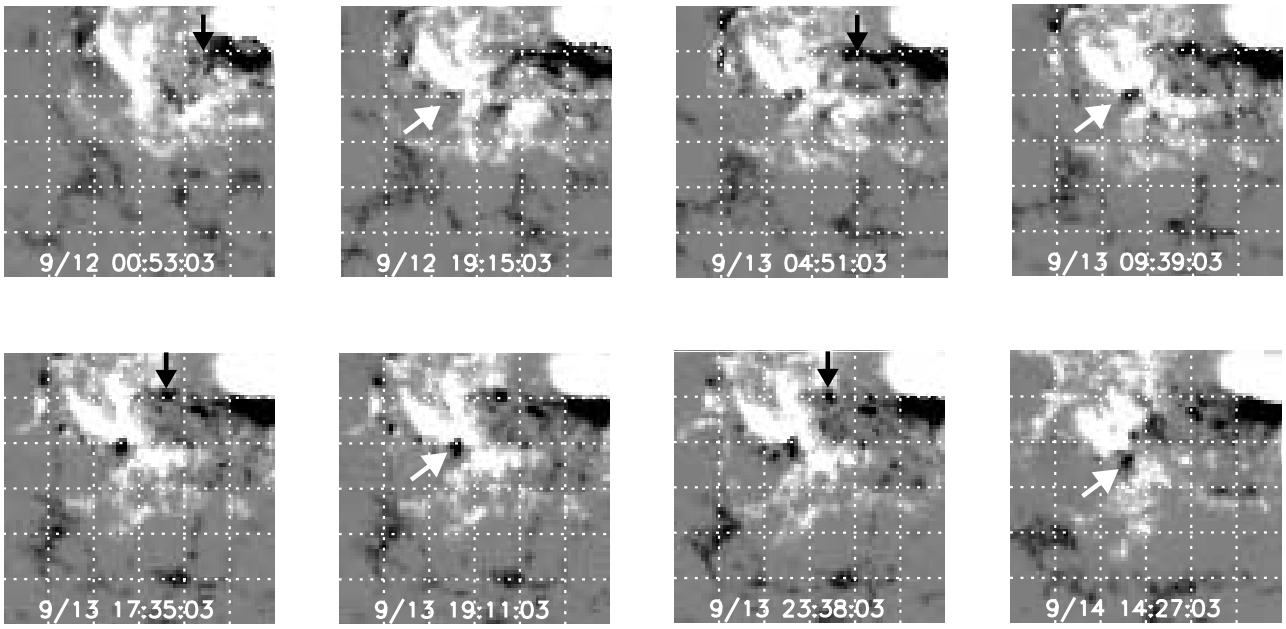

FIG. 12.—*SOHO* MDI magnetic maps showing the evolution of the magnetic field around the S-shaped neutral line. The area covered by each image is 150″ square, which corresponds to the square drawn in Fig. 6*b*. Dotted lines are drawn every 25″ (1.8×10^4 km). Black arrows indicate the negative elements in region C flowing out from the negative umbra in the delta-type spot, while white arrows indicate the negative elements emerging into region T and moving toward the footpoint of the loop that brightened along with the C2.9 flare at around 19:00 UT on September 13.

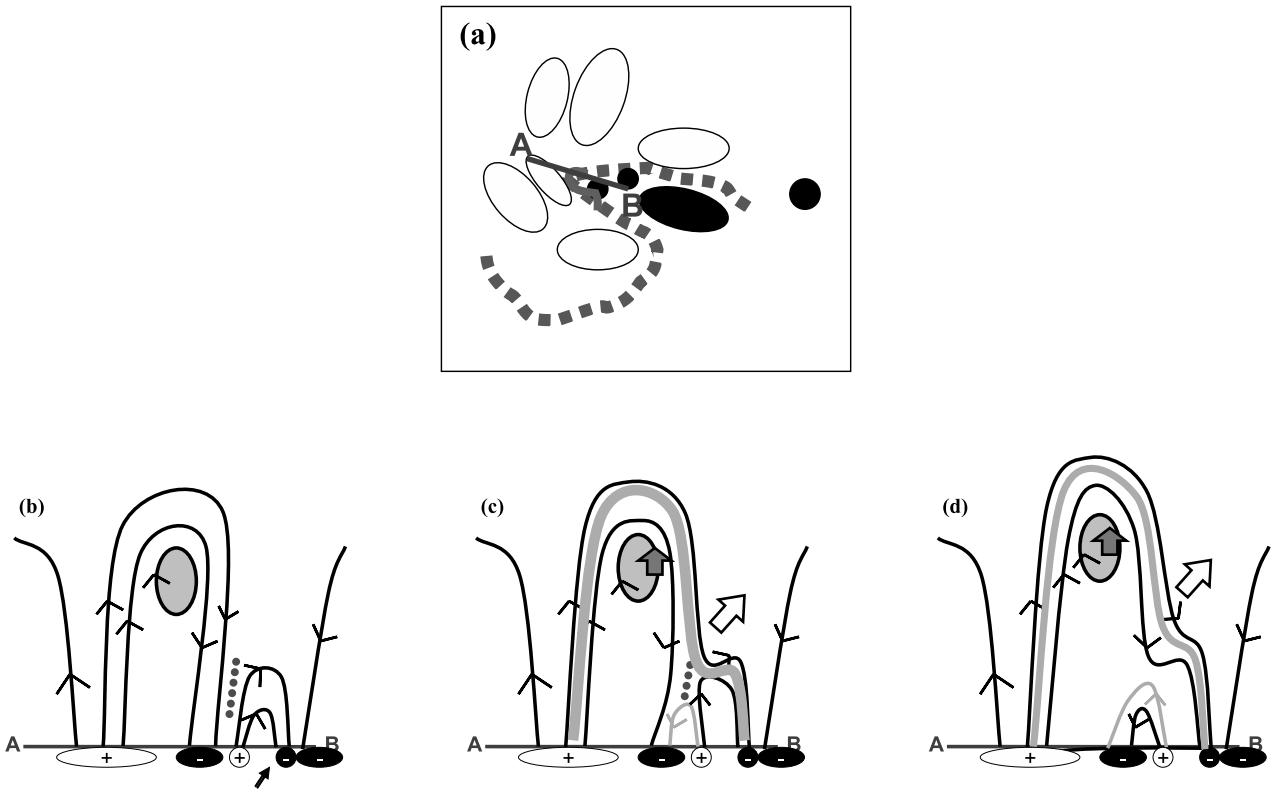

FIG. 13.—Schematic illustration of the evolution of magnetic structure at the time of flares in region C (group II; see Fig. 6*d*). This figure is based on the data of the M6.1 flare on September 12 as a representative of the flares in region C. However, we believe that all the flares in region C occurred in a similar way. (*a*) Simple sketch of magnetic structure in the active region when the flare occurred. White and black indicate positive and negative polarities. The dashed line indicates the S-shaped neutral line, and the gray curve on the neutral line indicates the filament in region C. (*b*) Cross section of magnetic structure along line AB shown in Fig. 13*a*. Solid lines are magnetic field lines, and the shaded area indicates the filament. The negative element indicated by an arrow is considered to be the key to this event. Between the field line connected to the element and the loops overlying the filament a current sheet forms (*dotted line*). Note that the positive element on the left side of the pointed negative element was not on line AB in reality; we consider that it was located on the positive side of the delta-type spot. (*c*) In the current sheet, magnetic reconnection occurred, and the loops overlying the filament brightened and were lengthened. The bright loop is indicated by the thick curve. The gray arrow indicates an ascending motion of the filament. (*d*) As the reconnection proceeds, arcades with increasing height allow the filament to ascend.

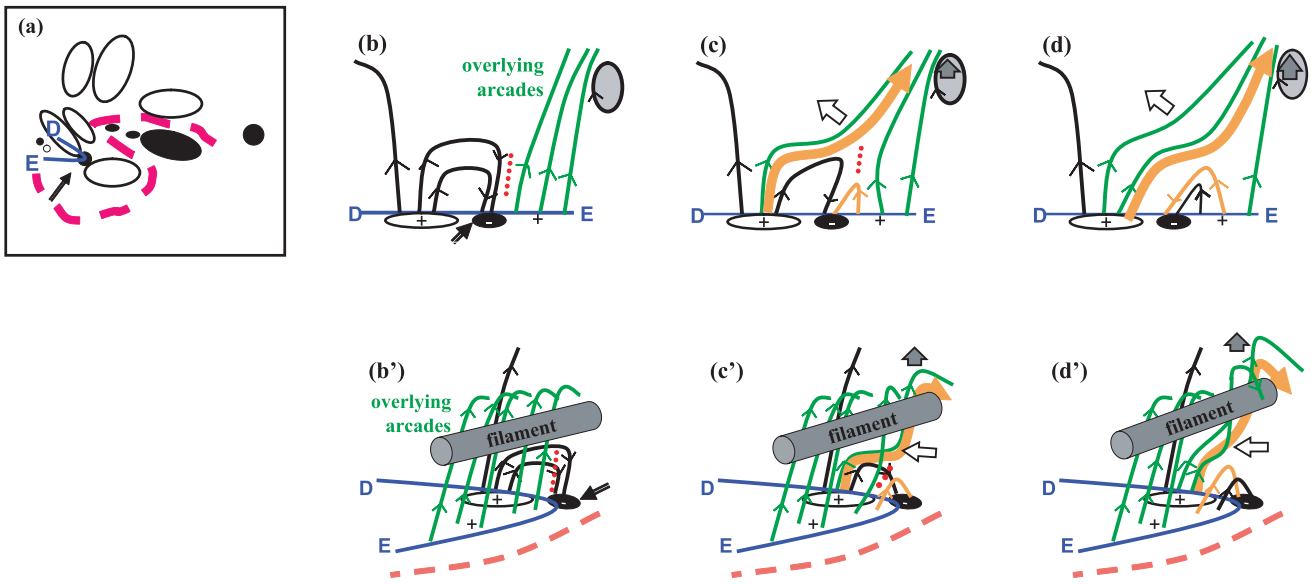

FIG. 14.—Schematic illustration of the evolution of magnetic structure at the time of flares in region T (group III; see Fig. 6*d*). This figure is based on the data of the C2.9 flare on September 13 as a representative of the flares in region T. (*a*) Simple sketch of magnetic structure in the active region when the flare occurred. White and black indicate positive and negative polarities. The dashed line indicates the S-shaped neutral line. (*b*) Cross section of magnetic structure along curve DE shown in Fig. 14*a*. In Figs. 14*b*–14*d*, curve DE is unbent in a straight line. The negative element indicated by the arrow is considered to be the key to this event. This element emerged into region T and moved toward the southwest. The shaded area indicates filament 2. Between the overlying loops and the emerging flux a current sheet formed (*red dotted line*). (*c*) In the current sheet, magnetic reconnection occurred. A small bright loop (*thin orange curve*) appeared as the left footpoint put on the negative element. The overlying arcade was lengthened, and the filament anchored by the arcade ascended as indicated by the gray arrow. A bright jetlike feature indicated by the orange arrow showed a whiplike motion as the loop stretched. The white arrow indicates this whiplike motion. (*d*) As the reconnection proceeded, jets with whiplike motion gradually moved eastward and the filament continued to move upward. (*b′*) Three-dimensional schematics of the magnetic structure along curve DE. Green lines indicate loops overlying filament 2, indicated by a gray cylinder. (*c′*) This panel shows the same phase as Fig. 14*c*. (*d′*) This panel shows the same phase as Fig. 14*d*.

small flares triggered the filament eruption through the process of lengthening the overlying arcade by magnetic reconnection. This is consistent with the emerging flux-triggering mechanism suggested by Chen & Shibata (2000) in that magnetic reconnection that occurred in a filament channel triggers a filament eruption. Note that Wang & Shi (1993) also suggested two-step magnetic reconnection: the first step of reconnection is a slow reconnection in the lower atmosphere that is observed as flux cancellation, while the flare energy release comes directly from the second step of reconnection that is the fast reconnection higher in the corona. However, the fact that many small flares occurred around the footpoints of filaments but that no eruption except the M6.1 flare on September 12 (feature [2] described above) was observed indicates that magnetic reconnection at the footpoints of filaments is not a sufficient condition for the eruption. In order to trigger the eruption, such a reconnection must occur when the filament is close to the critical point for loss of equilibrium; this is why the relatively small (C2.9) flare could trigger the eruption. Since in the initial condition of the simulation of Chen & Shibata (2000) the flux rope was already set in an equilibrium state very close to instability or loss of equilibrium, once magnetic flux emerges, the flux rope can erupt immediately. A loss-of-equilibrium model was proposed by Forbes (1990) and Forbes & Isenberg (1991). Forbes (1990) confirmed by a numerical simulation that when the filament current exceeds a critical value, the stable configuration containing the filament loses equilibrium and the filament may erupt. We suggest that the slow and long-lasting ascending motion of the filament presented in this paper corresponds to the change of the equilibrium height of the filament; the filament approaches the critical point from an initially stable equilibrium, as described in the loss-of-equilibrium model. For our X1.5 event, such change was due to the series of small flares involving the overlying arcade of the filament.

It has to be mentioned that we can interpret these processes in another way. In Figure 15 we show the structure of the C2.9 flare that occurred right before the X1.5 event. In this scenario, we consider that the moving magnetic elements played the key role in triggering the filament eruption; at the footpoint of the flux rope labeled as filament 2, reconnection occurred, and it made the flux rope itself lengthen directly. Then filament 2 erupted, and filament 1—which was already approaching certain critical point—also erupted as a result of the eruption of filament 2.

Another interesting feature to be noted here is a rising motion of bright structure during the slow rise of the filament indicated by an arrow in the time slice shown in Figure 7. This rising structure corresponds to an apparently swelling loop in the *TRACE* image. This may be related to a "bugle," which was reported by Hundhausen (1993). Bugles were observed as brightening and swelling of the bright belt of coronal streamers several days before a CME, and they suddenly disappeared as the CMEs occurred. They were named so because the shape looks like a bugle on synoptic maps at a given height in the corona. The timescale of bugles is the same order as the slow swelling motion in the corona found in our event, although the size of the bugle is much larger. Perhaps the swelling motion is the lower coronal counterpart of a bugle. One of the bugles reported by Hundhausen (1993) was investigated by Feynman & Martin (1995). During the development of the bugle, a new magnetic flux was observed to emerge below the large-scale arcades. As Chen & Shibata (2000) suggested, an emerging flux can trigger filament eruptions through the reconnection with the magnetic field lines around the filament. In our event, we found systematic motions of magnetic elements below the filament. Such moving magnetic elements may or may not be related to newly emerging fluxes, but they also can induce the magnetic reconnection that changes the equilibrium

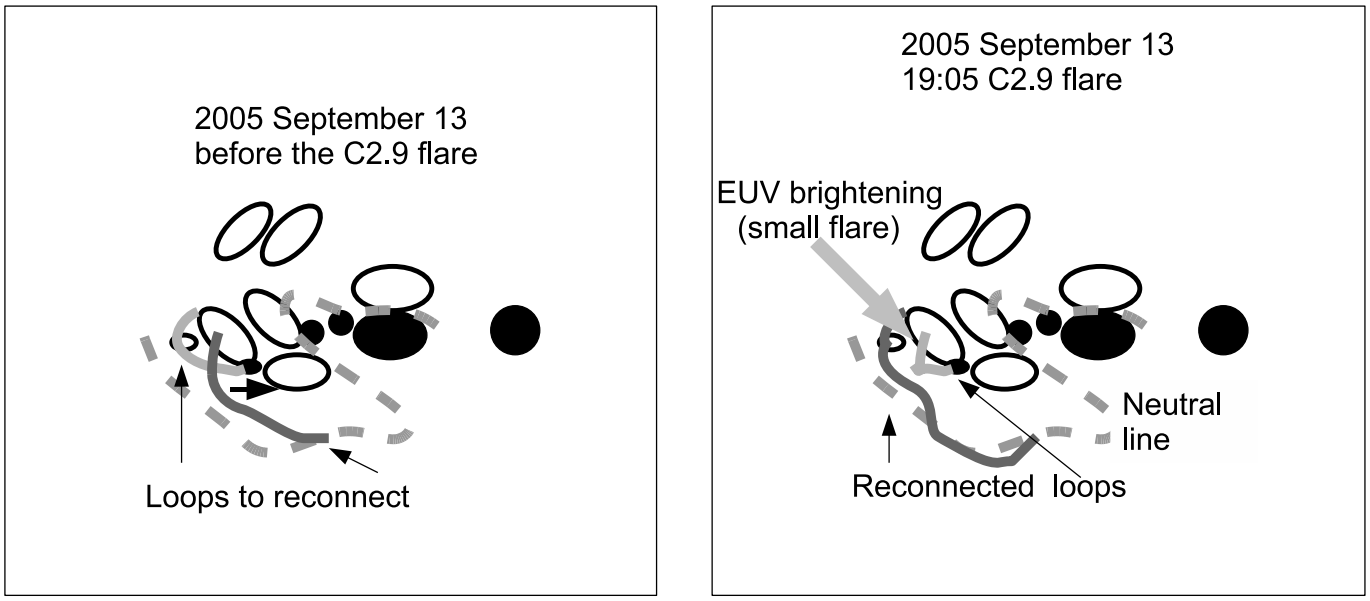

FIG. 15.—Alternative interpretation of the C2.9 flare at 19:05 UT on September 13. White and black indicate positive and negative polarities. The dashed line indicates the S-shaped neutral line. In the left panel, two magnetic lines crossed each other; this is the view before the small flare. As the negative polarity elements moved westward, the light gray magnetic line was pressed against the dark gray line and finally they reconnected (*see the right panel*). This dark gray line indicates filament 2, and owing to the reconnection it became longer. Therefore, filament 2 could not be held, and it erupted with filament 1.

state of the filament and triggers its eruption. Therefore, we suggest that (1) both emerging fluxes and moving magnetic elements in the vicinity of the filament neutral line can lead a filament to approach the loss of equilibrium, and (2) both the bugles in the high corona and the swelling loops in the low corona are the manifestations of the evolution of the coronal field that is approaching a loss of equilibrium (eruption).

Using multiwavelength data of these events, such as *TRACE* EUV 195 and 1600 Å data, MDI magnetograms, and BBSO and SMART Hα data, we tried to investigate extensively what happened in the active region before the filament eruption. Although we find several interesting features, we cannot definitively conclude what directly triggers such flares in the active region, since the magnetic structure of flares was extremely complex in this region. It is not clear whether one can know the equilibrium properties of a filament (flux rope) from a "snapshot" of the active region by, e.g., nonlinear force-free extrapolation of a photospheric magnetogram. Such approaches may work, but it is possible that one needs the evolutionary history of the active region for accurate diagnostics. Comparison of coronal observations and the numerical models of the coronal field calculated from observed magnetograms has been done extensively (e.g., Yan & Sakurai 1997). We stress the importance of studying the long-term (namely, more than a few days) temporal evolution of the photospheric and coronal magnetic field that eventually produces an eruption. The Solar Optical Telescope on board the *Hinode* satellite obtains accurate vector magnetograms with uninterrupted observation and therefore will provide ideal data sets for this purpose.

7. CONCLUSION

NOAA Active Region 10808 appeared in 2005 September and exhibited extraordinary flare activity that was the most active in solar cycle 23. Using EUV, Hα, and magnetogram data taken before and during eruptive events accompanied by an X1.5 flare (the X1.5 event), we investigate the processes leading to the catastrophic eruption. We find several interesting features that help us understand the physical mechanism of the X1.5 event. The main points are as follows.

1. The filament that erupted during the X1.5 event slowly ascended over 2 days before its eruption. The speed of the ascending motion was approximately 0.1 km s^{-1}.
2. While the filament was ascending slowly, many M- and C-class flares were observed close to the footpoints of the filament. At the sites where the flares frequently occurred, magnetic elements emerged and moved distinctively.

On the basis of these observational facts, we discuss the triggering mechanism of the filament eruption on 2005 September 13. We suggest that many small flares that occurred in the vicinity of the filament played a role in changing the topology of the magnetic field lines overlying the filament through small-scale reconnection. Over 2 days, they changed its equilibrium state gradually and allowed the filament to ascend slowly. In the end, a C2.9 flare that occurred just before the X1.5 event was considered to directly lead to the catastrophic filament eruption.

This work is supported by the Grant-in-Aid for the 21st Century COE "Center for Diversity and Universality in Physics" from the Ministry of Education, Culture, Sports, Science and Technology (MEXT) of Japan, and by the Grant-in-Aid for Creative Scientific Research "The Basic Study of Space Weather Prediction" (17GS0208; Head Investigator: K. Shibata) from MEXT. K. N., H. I., and T. J. O. are supported by the Research Fellowship from the Japan Society for the Promotion of Science for Young Scientists. *TRACE* is a NASA Small Explorer mission. *SOHO* is a project operated by the European Space Agency and the US National Aeronautics and Space Administration. We thank the Big Bear Solar Observatory for providing access to Hα data. Data analysis was carried out on the computer system at the Nobeyama Solar Radio Observatory of the National Astronomical Observatory of Japan.

REFERENCES

Antiochos, S. K., Dahlburg, R. B., & Klimchuk, J. A. 1994, ApJ, 420, L41
Antiochos, S. K., DeVore, C. R., & Klimchuk, J. A. 1999, ApJ, 510, 485
Asai, A., Ishii, T. T., Shibata, K., & Gopalswamy, N. 2006, in Solar Active Regions and 3D Magnetic Structure (Paris: IAU), 3
Chen, P. F., & Shibata, K. 2000, ApJ, 545, 524
Chifor, C., Mason, H. E., Tripathi, D., Isobe, H., & Asai, A. 2006, A&A, 458, 965
Chifor, C., Tripathi, D., Mason, H. E., & Dennis, B. R. 2007, A&A, in press
Feynman, J., & Martin, S. F. 1995, J. Geophys. Res., 100, 3355
Forbes, T. G. 1990, J. Geophys. Res., 95, 11919
———. 2000, J. Geophys. Res., 105, 23153
Forbes, T. G., & Isenberg, P. A. 1991, ApJ, 373, 294
Hale, G. E., Ellerman, F., Nicholson, S. B., & Joy, A. H. 1919, ApJ, 49, 153
Handy, B. N., et al. 1999, Sol. Phys., 187, 229
Hundhausen, A. J. 1993, J. Geophys. Res., 98, 13177
Isobe, H., & Tripathi, D. 2006, A&A, 449, L17
Isobe, H., Tripathi, D., Asai, A., & Jain, R. 2007, Sol. Phys., submitted
Kahler, S. W., Moore, R. L., Kane, S. R., & Zirin, H. 1988, ApJ, 328, 824
Lin, J., Forbes, T. G., & Isenberg, P. A. 2001, J. Geophys. Res., 106, 25053
Low, B. C. 1996, Sol. Phys., 167, 217
Martin, S. F. 1980, Sol. Phys., 68, 217
Moore, R. L., & Roumeliotis, G. 1992, in IAU Colloq. 133, Eruptive Solar Flares, ed. Z. Svestka, B. V. Jackson, & M. E. Machado (Berlin: Springer), 69
Ohyama, M., & Shibata, K. 1997, PASJ, 49, 249
Priest, E. R., Hood, A. W., & Anzer, U. 1989, ApJ, 344, 1010
Rompolt, B. 1990, Hvar. Obs. Bull., 14, 37
Scherrer, P. H., et al. 1995, Sol. Phys., 162, 129
Shibata, K., Masuda, S., Shimojo, M., Hara, H., Yokoyama, T., Tsuneta, S., Kosugi, T., & Ogawara, Y. 1995, ApJ, 451, L83
Shibata, K., Nitta, N., Strong, K. T., Matsumoto, R., Yokoyama, T., Hirayama, T., Hudson, H., & Ogawara, Y. 1994, ApJ, 431, L51
Sterling, A. C., & Moore, R. L. 2004, ApJ, 613, 1221
UeNo, S., Nagata, S., Kitai, R., & Kurokawa, H. 2004, in ASP Conf. Ser. 325, The Solar-B Mission and the Forefront of Solar Physics, ed. T. Sakurai & T. Sekii (San Francisco: ASP), 319
Wang, H., Liu, C., Jing, J., & Yurchyshyn, V. 2007, ApJ, submitted
Wang, J., & Shi, Z. 1993, Sol. Phys., 143, 119
Wang, Y., Xue, X., Shen, C., Ye, P., Wang, S., & Zhang, J. 2006, ApJ, 646, 625
Wang, Y.-M., & Sheeley, N. R., Jr. 1999, ApJ, 510, L157
Yan, Y., & Sakurai, T. 1997, Sol. Phys., 174, 65
Yashiro, S., Gopalswamy, N., Michalek, G., St. Cyr, O. C., Plunkett, S. P., Rich, N. B., & Howard, R. A. 2004, J. Geophys. Res., 109, 7105
Zhang, J., Dere, K. P., Howard, R. A., Kundu, M. R., & White, S. M. 2001, ApJ, 559, 452